THE JOURNAL OF COMPARATIVE NEUROLOGY 450:153–166 (2002)

Morphometric Analysis of Dendritic Remodeling in an Identified Motoneuron During Postembryonic Development

FREDERIC LIBERSAT[1]* AND CARSTEN DUCH[2]
[1]Zlotowski Center for Neuroscience and Department of Life Sciences, Ben Gurion University of the Negev, Beer Sheva 84105, Israel
[2]Fachbereich Chemie, Biologie und Pharmazie der Freien Universitat Berlin, Institute of Neurobiology, 14195 Berlin, Germany

ABSTRACT

A detailed quantitative description of modifications in neuronal architecture is an important prerequisite to investigate the signals underlying behaviorally relevant changes in neuronal shape. Extensive morphological remodeling of neurons occurs during the metamorphosis of holometabolous insects, such as *Manduca sexta*, in which new adult behaviors develop postembryonically. In this study, a morphometric analysis of the structural changes of an identified *Manduca* motoneuron, MN5, was conducted by sampling its metric parameters at different developmental stages. The remodeling of MN5 is divided into three main phases. The regression of most larval dendrites (1) is followed by the formation of dendritic growth-cones (2), and subsequently, adult dendrite formation (3). In contrast, the cell body and link segment surface increase during dendritic regression and regrowth, indicating that different cell compartments receive different signals, or respond differently to the same signal. During dendritic growth-cone formation, the growth of the cell body and the link segment are arrested. Sholl and branch frequency analysis suggest two different modes of dendritic growth. During a first growth-cone-dependent phase, new branch formation occurs at all dendrites. The maximum path length of the major dendritic tree changes little, whereas branch order increases from 20 to 45. Changes in total dendritic length are correlated with strong changes in the number of nodes but with minor changes in the average dendritic segment length, indicating a mode of growth similar to that induced by steroid hormone application to cultured motoneurons. The second phase is growth-cone-independent, and branching is limited to high order dendrites. J. Comp. Neurol. 450:153–166, 2002.

Indexing terms: dendrites; metamorphosis; insect; steroid hormones; ecdysteroids; growth cone

The development and plasticity of behavior must ultimately be understood on the level of cellular changes in the central nervous system. Adequate mature activity patterns rely on the correct differentiation of neuronal structure owing to the dual function of neuronal architecture. First, dendritic structure is important for the establishment of the correct pre- and postsynaptic connections, and thus, for the wiring of neuronal networks. Second, dendritic structure strongly influences the integration of synaptic input and neuronal firing properties (Mainen and Sejnowski, 1996).

Among the classes of molecules that have profound effects on neuronal structure are steroid hormones (Arnold and Gorski, 1984). They mediate changes in neuronal morphology in such diverse regions of the vertebrate central nervous system as the spinal motor nuclei, the hippocampus, and the supraoptic nucleus. These can be cor-

Grant sponsor: the Israel Science Foundation; Grant number: 335/00-1; Grant sponsor: the Yael Foundation; Grant sponsor: NIH; Grant number: NS28495; Grant sponsor: the Deutsche Forschungsgemeinschaft; Grant numbers: DU 331/2-1 and DU331/2-2.

*Correspondence to: Frederic Libersat, Department of Life Sciences, Ben Gurion University of the Negev, POB 653, Beer Sheva 84105, Israel. E-mail: libersat@bgumail.bgu.ac.il

Received 8 November 2001; Revised 29 January 2002; Accepted 9 May 2002

DOI 10.1002/cne.10318

Published online the week of July 8, 2002 in Wiley InterScience (www.interscience.wiley.com).

related temporally with the maturation and the seasonal variability in reproductive behavior, as well as with variations in learning and memory that correspond to stages of the estrous cycle, stress, and aging (De Voogd and Nottebohm, 1981; Kurz et al., 1991; Murphey and Segal, 1996; Stern and Armstrong, 1998). Besides hormone-induced modifications of motoneurons, interactions with synaptic partners (Catalano and Shatz, 1998; Penn and Shatz, 1999) or with the developing target muscles may play a role (Kent and Levine, 1993; Fernandes and Keshishian, 1998). Furthermore, there may be a functional interplay between changes in membrane currents and dendritic architecture (Duch and Levine, 2000), as is the case during embryonic development (Spitzer, 1991; Spitzer et al., 1994; Gomez et al., 1995; Gu and Spitzer, 1995; Gomez and Spitzer, 1999).

Holometabolous insects undergo dramatic morphological and behavioral changes during metamorphosis (Weeks and Levine, 1990, 1995; Consoulas et al., 2000; Tissot and Stocker, 2000) to accommodate the new adult behaviors. During the metamorphosis of the tobacco hornworm, *Manduca sexta*, ecdysteroids exert direct effects on motoneurons (Levine and Weeks, 1996). They influence dendritic regression and regrowth of motoneurons that are respecified during metamorphosis, and they also control the programmed cell death of motoneurons that are not needed for adult behavior (Weeks and Truman, 1985; Weeks, 1987; Weeks and Ernst-Utzschneider, 1989; Streichert et al., 1997). In cultured motoneurons, they induce increases in calcium membrane currents (Gruenewald and Levine, 1998) and enhance neurite branching by altering the growth-cone structure at the level of the cytoskeleton (Prugh and Levine, 1992; Matheson and Levine, 1999). However, it is not clear which specific features of neuronal architecture are regulated by ecdysteroids in vivo, whether the ecdysteroid effects obtained in culture systems are sufficient to explain the postembryonic neuronal modifications observed in situ (Kent and Levine, 1993; Duch and Levine, 2000), and how hormones act in concert with other signals.

During *Manduca* metamorphosis, five larval crawling motoneurons are respecified to innervate the adult dorsal longitudinal flight muscle (Casaday and Camhi, 1976; Kammer and Rheuben, 1976; Duch et al., 2000).This change of function is accompanied by extensive modifications in membrane properties and dendritic architecture, both of which have been documented for one of these motoneurons, MN5 (Duch and Levine, 2000). As for other *Manduca* motoneurons, the loss of larval dendrites in MN5 is followed by the formation of prominent growth cones and rapid growth of dendrites. Because MN5 is individually identifiable throughout all stages of postembryonic development, it is suitable for analyzing the mechanisms underlying postembryonic modifications of neuronal structure.

A fundamental prerequisite to understanding the signals underlying developmental modifications in neuronal architecture is a detailed analysis of structural changes in vivo. In this study, we performed three-dimensional (3D) reconstructions of MN5 at different developmental stages followed by a quantitative metric analysis to address the following questions. First, do all compartments of the neuron follow the same time course of retraction and regrowth? Second, how do specific modes of neuronal growth correlate temporally with signals that are present in vivo at different developmental stages? Third, what features of the structural modification of MN5 can be accounted for by the effects that are induced when ecdysteroids are provided to cultured *Manduca* motoneurons? In addition, this study establishes a database to elucidate further the signals underlying postembryonic neuronal modifications in future experiments.

MATERIALS AND METHODS

Animals

Manduca sexta larvae, pupae, and adults were reared in a laboratory colony that has been housed at the University of Arizona since 1985. Larvae were grown on artificial diet (Bell and Joachim, 1976) under a 17-hour light/7-hour dark photoperiod at 26°C and 60% humidity. Both morphological and chronological criteria were used for the staging of the animals (Nijhout and Williams, 1974; Bell and Joachim, 1976; Reinecke et al., 1980; Tolbert et al., 1983). In summary, L5 represents an animal from the fifth larval instar (animals were used on day 2 of this larval stage), W0–W4 refer to the 5 days of wandering, and P0 refers to the first day of pupal life. Pupal life is divided into 18 stages (P1–P18), roughly corresponding to days. P18 represents the last day of pupal life before adult emergence. The experiments comply with Principles of Animal Care, NIH publication no. 86-23, revised in 1985, and also with the current laws of the State of Israel.

Staining of MN5

MN5 was stained intracellularly. Identification was achieved by antidromic stimulation pulses of 5 V amplitude and 0.5 msec duration, which were sufficient to evoke antidromic sodium spikes at all stages of postembryonic development (Duch et al., 2000). Rhodamine dextran (D3308; Molecular Probes, Eugene, OR) was injected iontophoretically with depolarizing current pulses (2 nA, 200 msec duration, 3/sec) for 30–120 minutes depending on the developmental stage. Then the electrode was removed and the preparation was left in saline for additional 10 minutes to allow dye diffusion. The ganglion was then washed in phosphate-buffered saline (PBS) buffer for 30 minutes, fixed in 4% paraformaldehyde for 2 hours, and dehydrated in ethanol (30, 50, 70, and 90%, two times 100% for 15 minutes each). Following dehydration, the ganglion was cleared slowly in methyl salicylate on a glass slide. Then methyl salicylate was carefully replaced with Permount (Fischer Scientific, Fair Lawn, NJ). The coverslip was placed carefully to avoid flattening. In other insects, this histological procedure induces mainly isometric shrinkage of about 15% of the total volume of the ganglion (Bucher et al., 2000). Therefore, morphometric parameters like neuronal volume and surface area should be affected isometrically within one stage, and similarly among different stages. This allows an adequate comparison of these parameters between different developmental stages. The results of this study do not depend on the absolute morphometric parameters, but on the relative differences between these values among different developmental stages.

Confocal microscopy

Digital images were captured on a Nikon PCM 2000 laser scanning confocal microscope using simple PCI

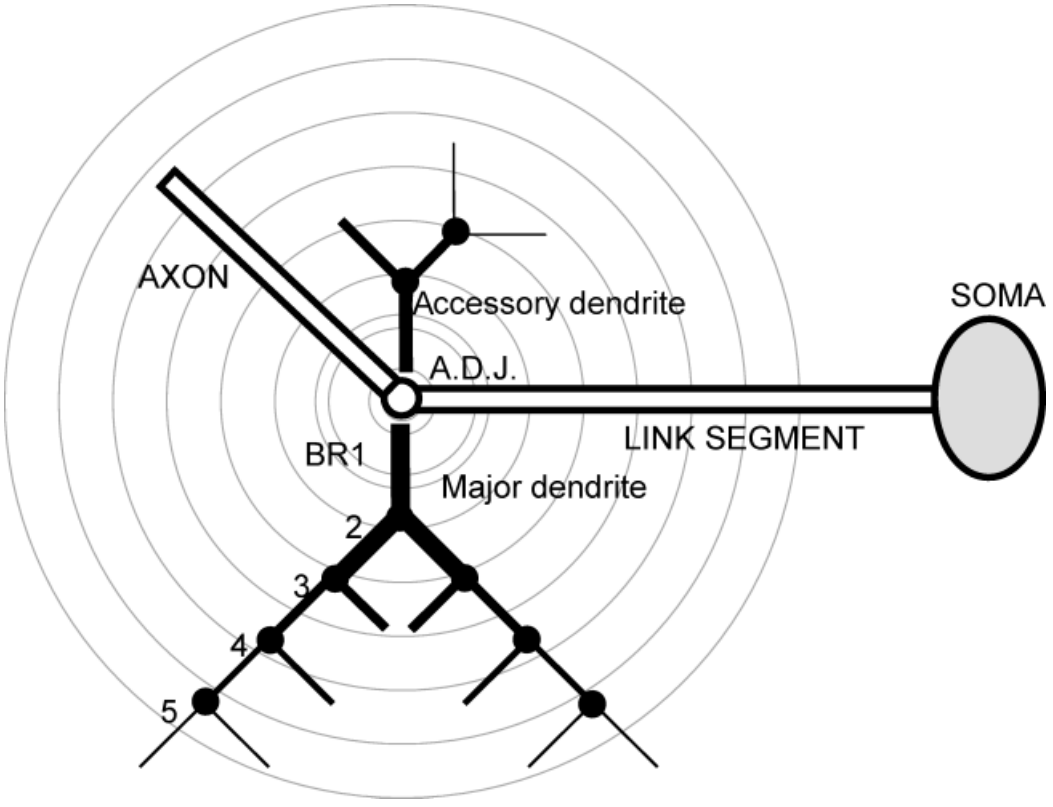

Fig. 1. General skeleton of MN5 and parameters used to describe the morphology of MN5. BR 1, branch order 1; node, branch point; ADJ, axon/dendrite junction. Specific parameters are quantified along the concentric circles used in the Sholl analysis or as a function of branch order (1–5).

(Compix, Cranberry Township, PA) as acquisition software. Preparations were scanned with a helium-neon laser line with an excitation maximum at 546 nm using a long-pass filter at 565 nm. All fields of view of MN5 in any given preparation were scanned at 1 μm optical sections with a 40× oil immersion lens (NA 1.0; working distance 180 μm). The distance between two pixels in the x and the y dimensions was 0.31 μm. No deconvolution was applied.

Reconstructions

The neurons were reconstructed with a commercial 3D system (Neurolucida; Microbrightfield, Williston, VT). For the 3D image acquisition of MN5 at different developmental stages, a series of optical sections of 1 μm thickness was acquired for each field of view (three to four fields). The image sequences were saved as TIFF files for subsequent 3D reconstruction. The portion of the neuron within a given field of view was reconstructed; then the tracing was exported and realigned in the x, y, and z dimensions to the next stack of images of the next field of view. Each fully reconstructed neuron consisted of a series of data points each of which was defined by the x, y, and z coordinates and the diameters of the tapered branch. The software Neuroexplorer (Microbrightfield) was used to compute various morphometric parameters.

Quantitative morphometry

MN5 is a monopolar neuron with a soma contralateral to the axon and dendritic tree (Figs. 1, 2). The soma is located outside the neuropil on the edge of the ganglion. It is connected to the axon and the dendritic tree by a neurite, which we refer to as the link segment. The segment of the dendrite from its origin at the link segment or the axo-dendritic junction to the first node is called a first order branch. The daughter branches arising from the first node are second order branches, and so on (Fig. 1). It is important to note that, with this method of branch order assignment, the addition of an interstitial branch would increase the order of all the more distal branches that had already been there. The branches arising from a common first order branch constitute a dendritic tree. In our reconstructions of MN5, each dendritic segment gives rise to two daughter branches at a node. There are several dendritic trees arising from the link segment. The longest of these extends anteroposteriorly from the axo-dendritic junction and is individually identifiable among different preparation from one stage or from different stages. We took advantage of this feature to analyze the changes in dendritic architecture during regression and regrowth of this dendrite. For clarity, we will refer to this dendrite as the major dendrite.

Several parameters of the structure of MN5 were examined quantitatively, including the length of the longest axis and surface area of the soma, the length and diameter of the link segment, the total dendritic length, the total dendritic surface area, the average dendritic segment length, the number of nodes, the maximum tree order, and the maximum path distance (Uyling et al. 1986). The

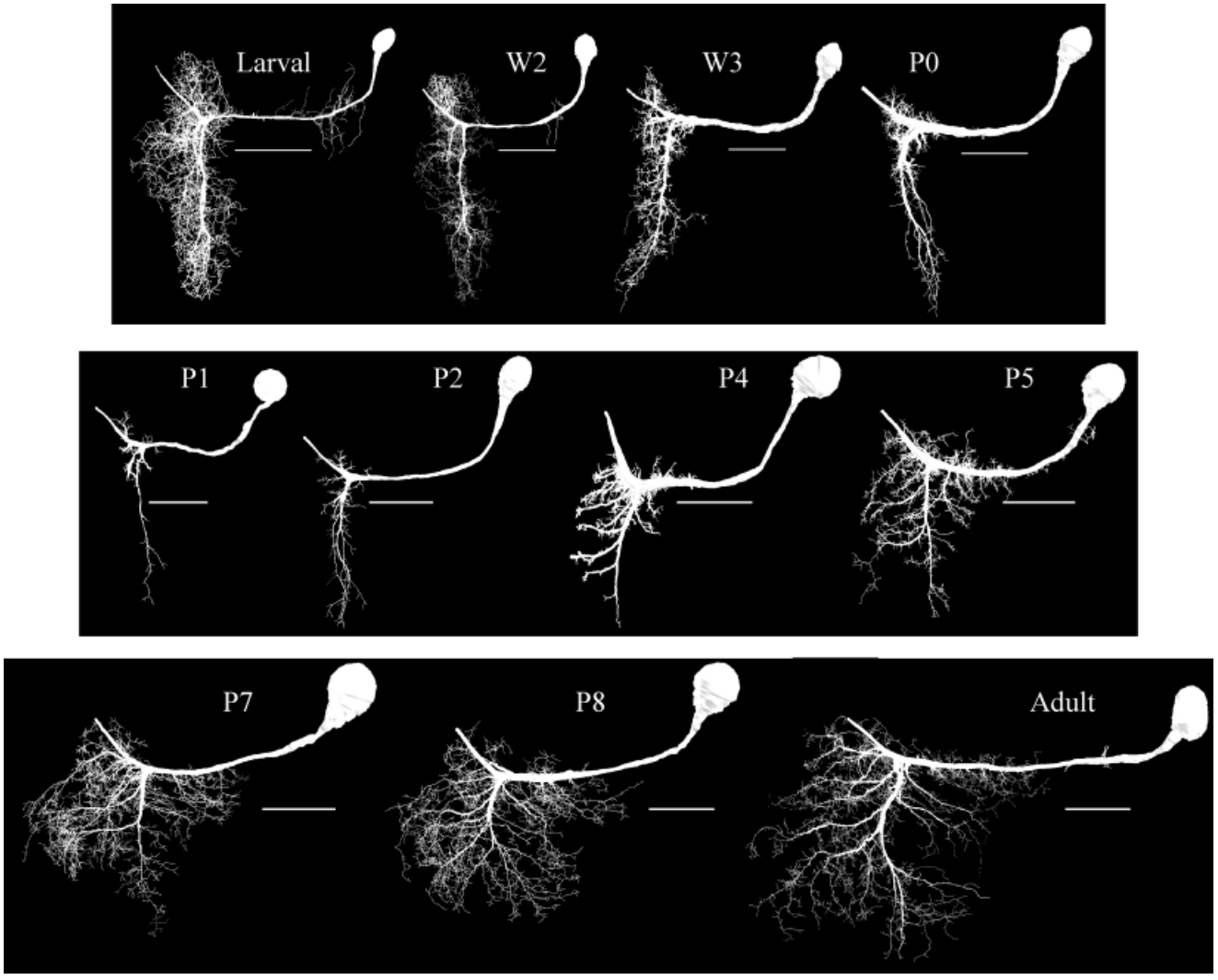

Fig. 2. Changes in the architecture of MN5 during development. Examples of the structure of MN5 at different developmental stages (11 stages are shown: W, wandering; P, pupae). Each neuron is a reconstruction from a stack of images taken with a confocal microscope. Scale bar = 100 μm for all stages.

length, surface area, and volume of the dendritic branches were calculated by equations provided by Microbrightfield software. These values were exported to Excel software (Microsoft) and used for further computations.

The Sholl analysis measures the occurrence of a given metric parameter between two consecutive spherical shells (Sholl, 1953). All neurons were aligned to the node between the link segment, axon, and the root of the major dendrite; then concentric spheres, spaced 20 μm apart, were centered at this alignment node (Fig. 1). The number of nodes within each sphere was measured.

RESULTS

In the present study, we have examined the dendritic remodeling of an identified motoneuron during postembryonic development by reconstructing 35 samples of MN5 at 14 different developmental stages.

Overall structural changes in MN5

MN5 undergoes severe dendritic regression during the end of larval and the first 2 days of pupal life (Duch and Levine, 2000) (Fig. 2). Dendritic regression is characterized by a significant loss of larval dendritic branches that starts at the second day of the wandering phase of the larval stage. Although the neuron loses many high order branches, the remaining branches become thicker and more compact compared with earlier larval stages (Fig. 2). The dendritic field reaches its maximum retraction during the pupal stages P1 and P2. The length of the major primary dendrite changes little (y-axis: larval 245 μm; W3 285 μm; P0 283 μm; P1 284 μm), whereas the width of the dendritic field decreases during dendritic regression (x-axis: larval 160 μm; W3 172 μm; P0 50 μm; P1 64 μm). The width of the dendritic tree in the z-axis changes little during dendritic

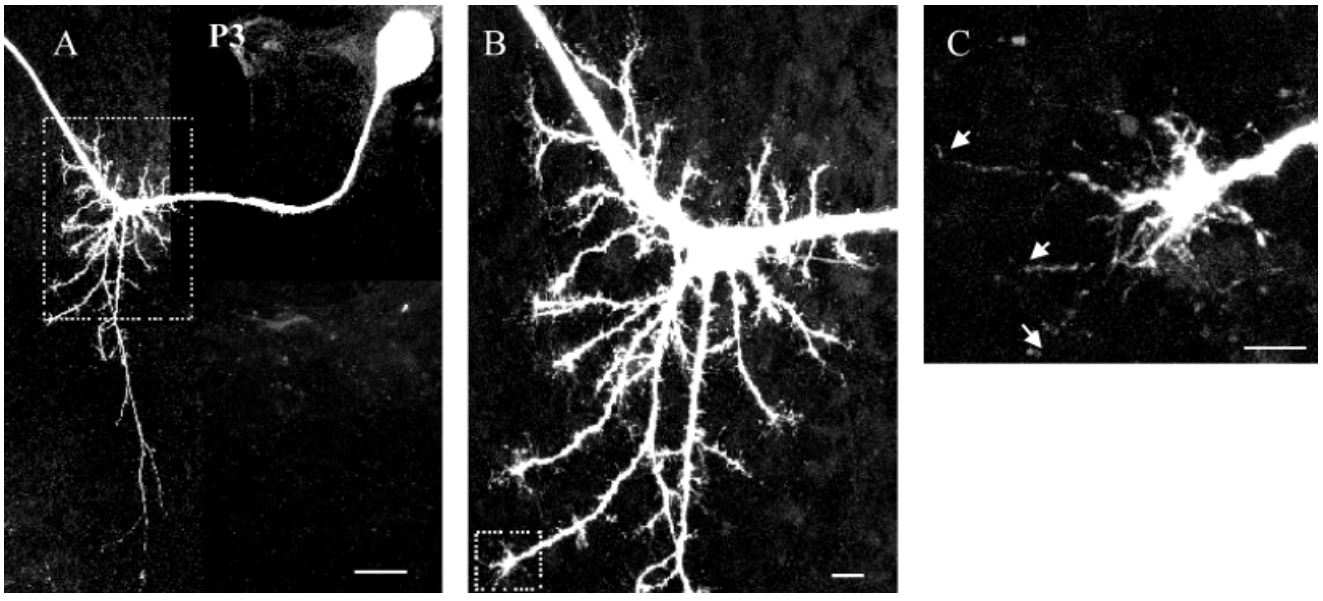

Fig. 3. Dendritic growth-cones. **A:** Extended focus image of an intracellular staining of MN5 at pupal stage P3. The dotted square indicates the dendritic region that is shown as a selective enlargement in **B**. Note that growth cones are located at the tips of all dendrites. The dotted square indicates a single growth cone that is selectively enlarged in **C**. Scale bar = 50 μm in A, 10 μm in B, 5 μm in C.

regression but decreases between P0 and P1 stages (larval 71 μm; W3 58 μm; P0 61 μm; P1 17 μm).

Dendritic regression is followed by the formation of prominent growth-cone–like structures at the tips of all remaining dendrites (Fig. 3). The peak abundance in growth-cone formation lasts for about 3 days (number of growth cones: pupal stage P3, 30 ± 9; P4, 44 ± 12; P5, 59 ± 20), but some growth cones are detectable until pupal stage P6. This coincides in time with an increase in the systemic ecdysteroid titers during early pupal life (Bollenbacher et al., 1981; Riddiford, 1985). Two weeks of growth and branching of new adult dendrites (Fig. 2) follow the initial growth-cone formation. During the formation of the adult dendritic field, many high order branches are formed, and the density of dendrites within the bounding borders of the dendritic field increases markedly (Fig. 2). The length of the major primary dendrite changes little (*y*-axis: P1, 284 μm; P2, 241 μm; P5, 215 μm; P8, 232 μm; adult, 332 μm), but the width of the dendritic field increases during dendritic growth (*x*-axis: P1, 64 μm; P2, 73 μm; P5, 151 μm; P8, 292 μm; adult, 387 μm). The width of the dendritic tree in the *z*-axis increases from P2 until adulthood (P1, 17 μm; P2, 15 μm; P3, 85 μm; P4, 134 μm; P5, 156 μm; P8, 162 μm; adult, 199 μm).

Developmental changes in neuronal morphology are not restricted to specific parts of the cell, but the architecture of all major cell compartments (dendrites, link segment, cell body) is changed during metamorphosis. As the size of the ganglion increases, the length of the link segment increases, so that the distance between the soma and the axo-dendritic junction, where the major dendrite branches off the link segment, is increased continuously during pupal life. Simultaneously, the size of the soma increases markedly. An overlap of representative reconstructions of MN5 from the three most extreme postembryonic developmental stages (larva, P1, adult) illustrates the drastic changes in the overall neuronal morphology. The length of the major dendrite changes very little; by contrast, the width of the dendritic field decreases threefold during regression and eightfold during regrowth (Fig. 4). The dramatic differences in tree structure among these three different developmental stages are illustrated by 2D dendrograms of the major dendrite (Fig. 5). The number of nodes decreases from roughly 1,850 at larval stage to 80 at the P1 stage and then increases to 2,500 in the adult stage.

Therefore, only 4% of the larval dendrites remain in the reduced dendritic field at stage P1. During regrowth, the number of dendrites increases 31-fold, and thus the adult dendritic field contains only 3% of the original larval dendrites. Accompanying this change in the number of nodes, the maximum branch order decreases from 77 in the larval stage to 18 at P1 stage and increases from 18 to 86 in the adult stage, showing that the complexity of the dendritic tree is rather similar in the larval and in the adult MN5 but that the adult tree contains mainly new dendritic branches.

Rotating MN5 around its *y*-axis reveals that the soma is offset from the dendritic arborizations in the *z*-axis (Fig. 6A). The dendritic tree occupies only 105 ± 40 μm (range among the different stages is 15–199 μm) in the *z*-axis. A comparison between reconstructions of MN5 from different animals of the same developmental stage indicates a relatively low morphological variability. The different preparations share a very similar dendritic geometry, although there is some variability in the precise dendritic branching patterns, which makes the identification of individual high order dendritic branches difficult (Fig. 6B). However, the variability of the main metric parameters, like the number of nodes and the surface area, is low enough to analyze the modes of growth of the different cell compartments quantitatively throughout all stages of

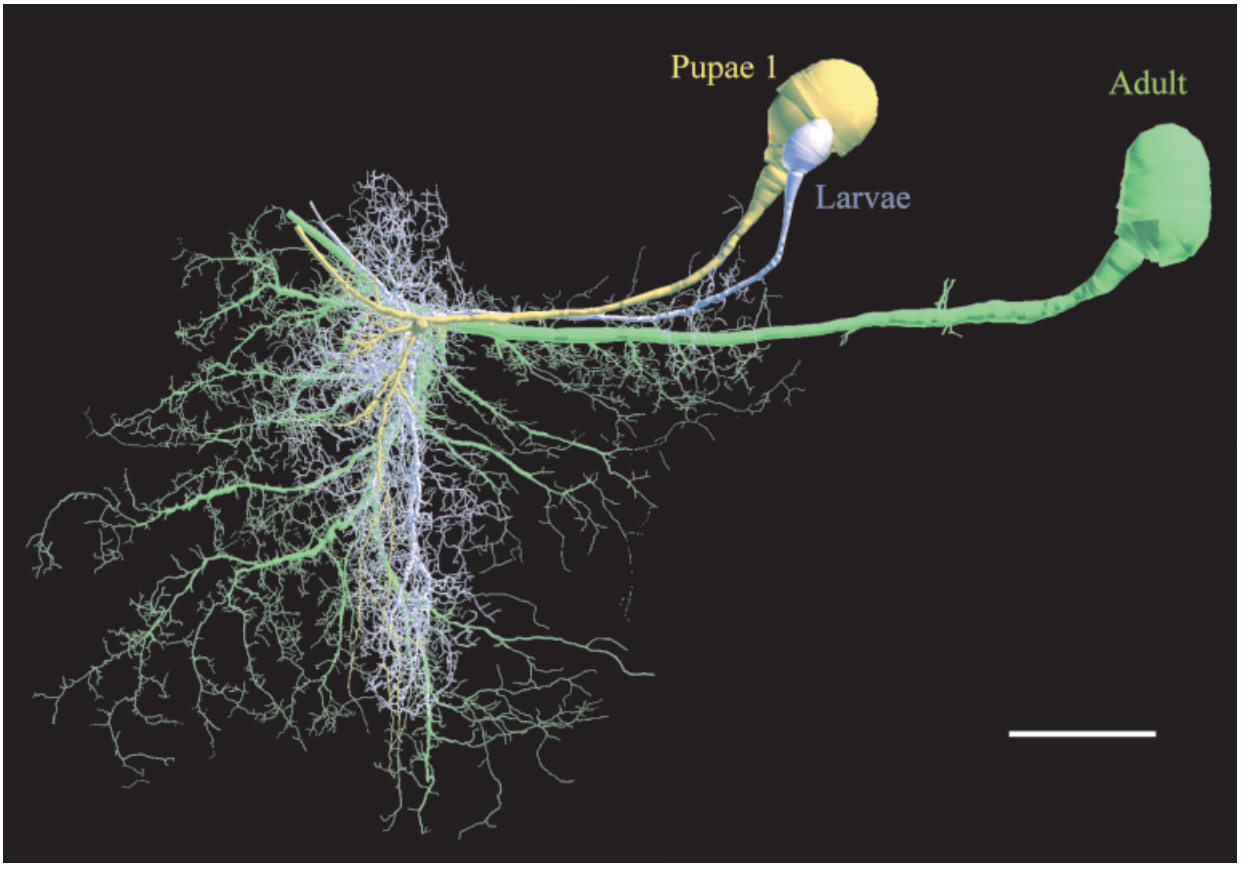

Fig. 4. The architecture of MN5 at three different developmental stages. The three examples of MN5 (larval stage in gold, pupal stage 1 in green, and adult stage in purple) and their respective dendritic tree are aligned to the axo-dendritic junction, illustrating the dramatic changes in the architecture of MN5 during remodeling. Scale bar = 50 μm.

postembryonic development. For instance, for P0 (n = 3) and P1 (n = 4), the number of nodes is 496 ± 68 (mean ± SD) and 78 ± 21 respectively, and the surface area is 21,351 ± 3,825 and 6,627 ± 306 μm^2, respectively. This shows that within just 1 day of postembryonic development, both the surface area and the number of dendrites change significantly (unpaired *t*-test; $P \leq 0.05$).

Different compartments of MN5 are modified with different time courses

The sizes of the soma and the link segment (n = 40) increase during both dendritic regression and dendritic growth (Fig. 7A). During dendritic regression, the length of the soma long axis increases by 60% from 38 ± 14 μm (L5) to 60 ± 7 μm (P0). In contrast, it remains relatively constant during the phase of the formation of growth cones (P1, 54 ± 19 μm; P2, 54 ± 12 μm; P3, 64 ± 6 μm; P4, 52 ± 15 μm). Then it increases again by 55% until P7 (93 μm) but does not change drastically between P7 and adulthood (82 μm). Likewise, during dendritic regression, the surface area of the link segment increases by 115% from L5 to P0. In contrast, it remains relatively constant during the phase of the formation of growth cones from P1 to P5 and increases again by 70% until the adult stage (data not shown). Thus, the changes in somatic (Fig. 7A) and link segment surface area follow the same time course.

Furthermore, the increases in soma and link segment sizes are nonlinear. The two growth periods during late larval and midpupal life are interrupted by a phase during early pupal life (P2–P4) that is characterized by the formation of dendritic growth cones. In contrast to the soma and the link segment, the dendritic surface area decreases during the end of larval life and the first 2 days of pupal life by a factor 8 from 53,160 μm^2 to 6,630 ± 306 μm^2 (Fig. 7B). From pupal stage P2 until adulthood, the dendritic surface area increases by a factor of 9.5 to reach a maximum of 63,140 μm^2. As a consequence of the modifications of the different compartments, the ratio of the dendritic to somatic membrane surface area is changed drastically during development (Fig. 7C). The larval dendritic tree decreases 30-fold during dendritic regression (0.7 for P2). In contrast, it increases only sevenfold during dendritic growth because the soma and the link segment also grow during this period. Therefore, the adult dendritic dominance is only 5 compared with the factor 20 in the larval MN5.

Changes in dendritic surface area are mainly caused by changes in the number of dendritic branches

Changes in dendritic surface area are paralleled by changes in the numbers of nodes (Fig. 8). An eightfold decrease in dendritic surface area from roughly 53,000

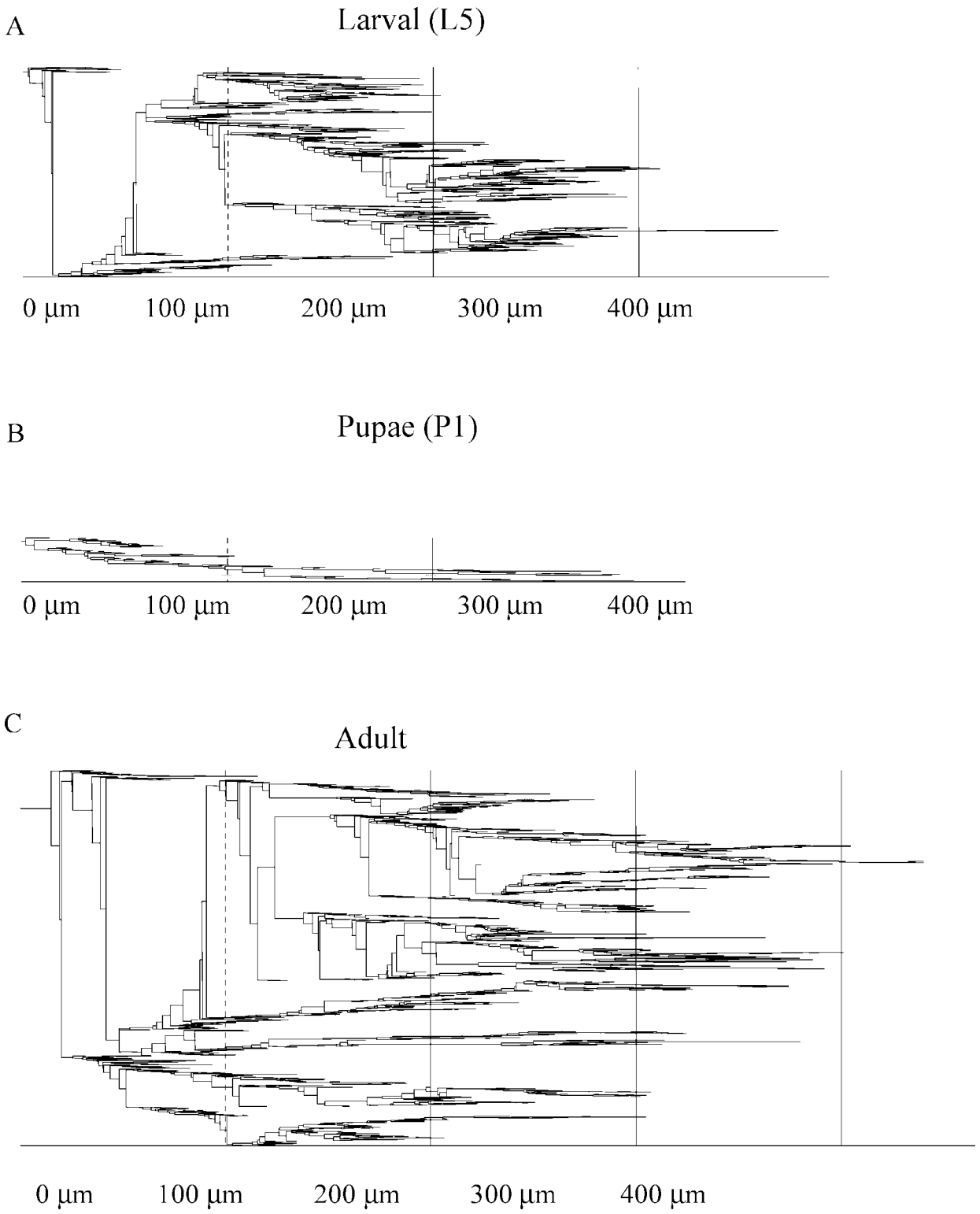

Fig. 5. **A–C:** Two-dimensional tree diagrams of the dendritic branching patterns of the major dendritic tree from reconstructions of MN5 at the three most different stages of postembryonic development (larva, P1, adult) that are shown in Figure 4. The origin of each tree diagram represents the root of the major dendrite that branches from the link segment. For each of the three developmental stages, each branch of the tree diagram resembles a dendritic branching point. The distance of each branching point and the length of each dendritic segment as measured along the path of the dendrite proximal to the node is indicated on the x-axis.

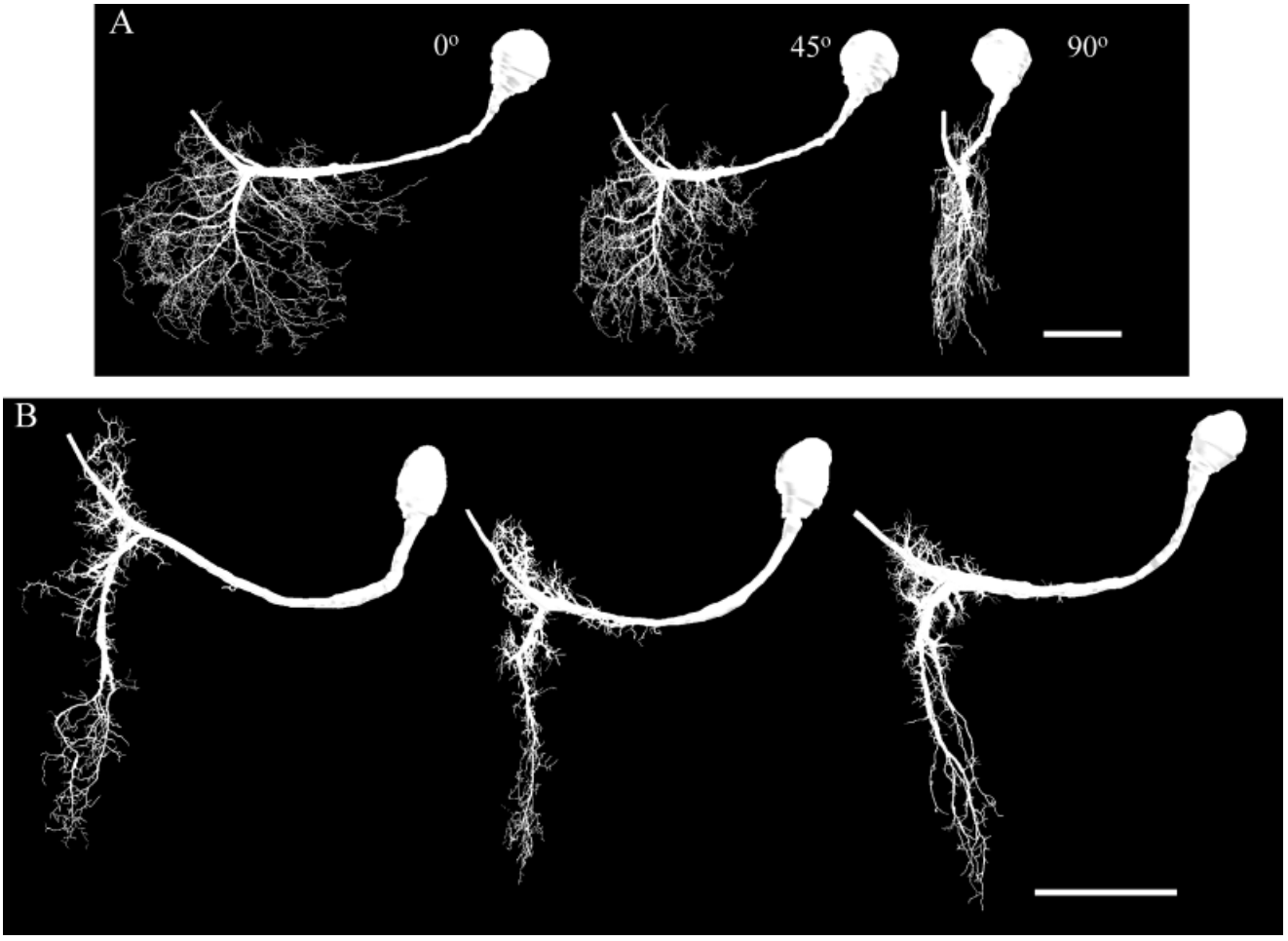

Fig. 6. **A:** Three different views of MN5 at pupal stage P8. The left image is a dorsal view of the neuron, the middle image is a dorsal view of the same neuron after a rotation of 45 degrees around the y-axis, and the right image is a dorsal view of the same neuron after a rotation of 90 degrees. **B:** Three examples of MN5 reconstructed from stainings from three different animals of the same developmental stage, pupal stage P0. Scale bar = 100 μm for all examples.

μm^2 to 6,500 μm^2 during retraction is accompanied by a 22-fold decrease in the number of nodes from 1,850 to 78 between the larval stage and pupal stage P1 (Fig. 8). During regrowth, a roughly 10-fold increase in dendritic surface area is accompanied by a 30-fold increase in the number of nodes from 78 to 2,490 (Fig. 8). Both the dendritic surface area and the number of nodes remain relatively constant during the formation of growth cones (P2–P4).

During regression, the decrease in the number of nodes is correlated with a decrease in the branch complexity of the dendrite (Fig. 8). For instance, a decrease in branch complexity is expressed as a decrease in the maximum branch order in the regressing dendritic tree from 77 in the larval MN5 to 18 ± 9 at the P1 stage (Fig. 8). During regrowth, the increase in the number of nodes is then correlated with an increase in branching order in the major dendritic tree. In addition, the maximum dendritic path length of the major dendrite decreases from 410 μm (L5) to 300 μm (P2) during regression and increases to 500 μm in the adult MN5. Therefore, the changes in the number of branches and in the branching order are also accompanied by changes in the length of the major dendrite, although the latter are less drastic by 1 order of magnitude.

The modes of dendritic retraction and growth

Growth of the dendritic tree clearly involves the addition of new dendritic segments (new nodes). Does it also involve a net elongation of the dendritic segments between nodes? The total dendritic length (TDL) was defined as the sum of the length of all dendritic segments. The mean dendritic segment length (MDL) was defined as the average length of all individual dendritic segments of the tree. Whereas changes in TDL are dramatic, changes in the MDL are relatively small during both retraction and regrowth (Fig. 9). TDL decreases 10-fold during regression and increases 16-fold during regrowth. In contrast, MDL increases and decreases twofold during regression and regrowth, respectively. This finding shows that the size of the dendritic field is mainly changed by a successive loss of dendritic segments during retraction and a successive addition of new adult segments during the initial growth

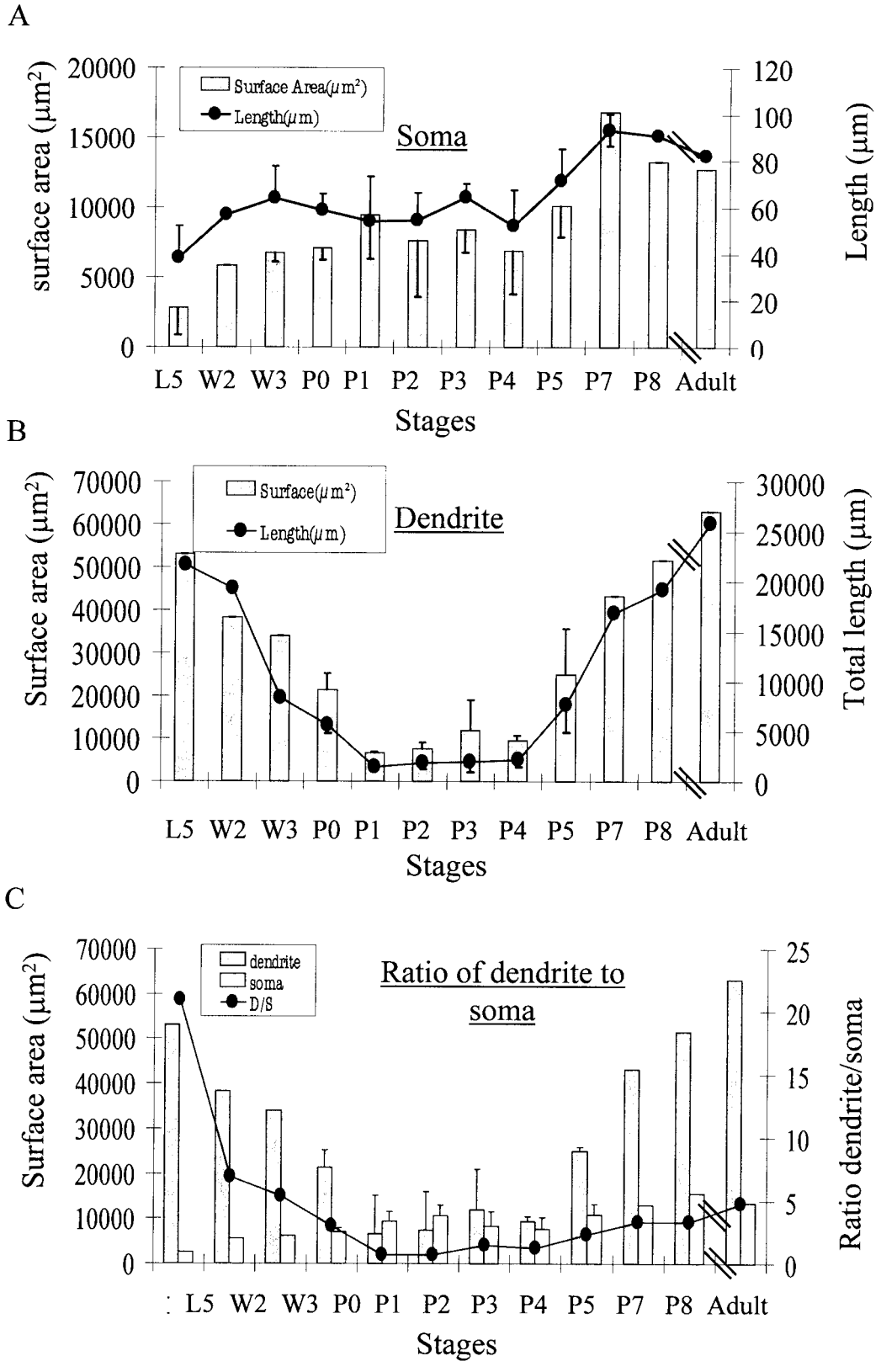

Fig. 7. Changes of the soma, the link segment, and the dendritic tree of MN5 during postembryonic development. **A:** Histogram of the soma surface area (gray bars) and line chart of the soma length throughout postembryonic development. **B:** Histogram of the dendritic surface area (gray bars) and line chart of the total dendritic length throughout postembryonic development. Both parameters decrease during late larval and early pupal life, remain unchanged during the pupal stages P1 to P4, and increase between pupal stage P4 and adulthood. **C:** Relative changes in the sizes of the soma and the dendrites of MN5 during postembryonic development. Histogram of the somatic (white bars) and the dendritic surface area (gray bars) throughout postembryonic development. Both compartments changes their sizes with different time courses, resulting in a change in the ratio of dendritic to somatic surface during development, as shown by the black line chart.

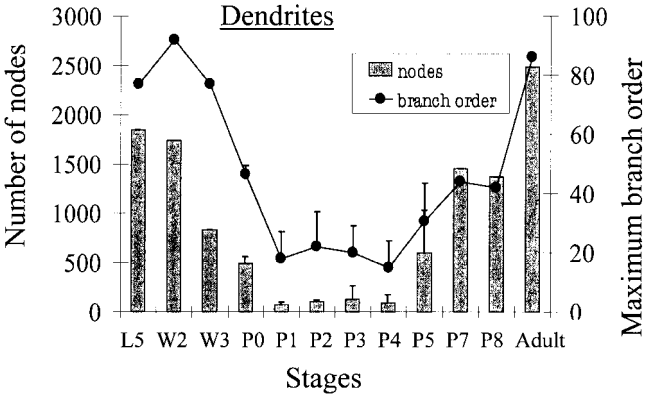

Fig. 8. Changes in the number of nodes and in branch order in the dendritic tree of MN5 during development. Bar graph showing the number of branching points (nodes) of the dendritic tree throughout postembryonic development (gray bars) and line graph showing the maximum branch order of the major dendritic tree throughout postembryonic development.

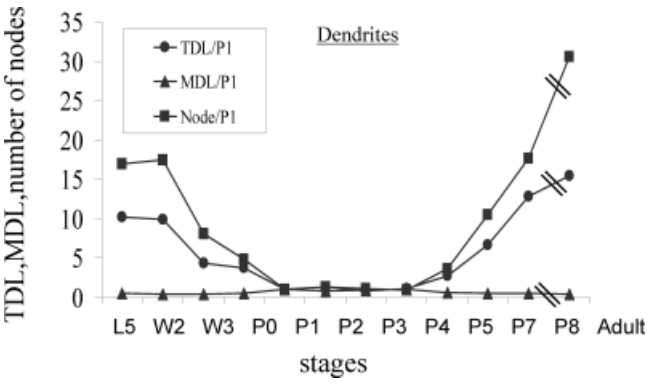

Fig. 9. Changes in quantitative branching parameters of the major dendrite during regression and regrowth. Line chart of the total dendritic length (TDL, circles), the mean dendritic length (MDL, squares) and the number of nodes (triangles) throughout postembryonic development. To allow a graphic comparison of these three parameters within one chart, all results were normalized to the P1 stage. The values of TDL, MDL, and number of nodes at the most regressed stage, pupal stage P1, were defined as 1. Both dendritic regression and dendritic growth are characterized by large changes in TDL and in the number of nodes, but MDL remains largely unchanged throughout development.

between pupal stages P1 and P8 rather than by major changes in the average length of the individual arborizations. Changes in TDL, MDL, and number of nodes are negligible during the phase of growth-cone formation between the pupal stages P1 and P4.

Most of the increase in TDL (1,200%) occurs during the initial phase of rapid dendritic growth between the pupal stages P4 and P8 (roughly 4 days in total). After about 50% of pupal life (at pupal stage P8), both the increase in the total dendritic length and the increase in the number of nodes are slowed down (Fig. 9). The remaining 21% of growth occurs during the second half of pupal life (roughly 10 days in total). Thus, the growth rate in TDL is significantly higher during the initial phase of dendritic growth than between pupal stage P8 and adulthood (Fig. 9).

Furthermore, between P4 and P8, MDL decreases from 12.2 ± 4.5 to 6.8 ± 1.6 μm and thus does not contribute to the rapid and large increase in TDL. Between P8 and adult, MDL further decreases from 6.8 ± 1.6 to 5 ± 1.3 μm and also does not contribute to the additional 21% of increase in TDL. Given these observations, we define two distinct phases of dendritic growth during pupal development. A first phase consists of rapid growth and branching between the pupal stages P4 and P8 (growth phase I) during which the increases in both TDL (88%) and nodes (18-fold) and the decrease in MDL (45%) are large. The first phase occurs in the presence of dendritic growth cones (Fig. 3) and is characterized by a strong and rapid increase of TDL that is achieved almost exclusively by new branch addition. The second phase (growth phase II) is characterized by a slower increase in TDL (20%) and nodes (0.75-fold) and is accompanied by a smaller decrease increase in MDL (27%) (growth phase II). The second phase occurs in the absence of growth cones.

To test further whether this division into two phases reflects qualitatively different modes of dendritic growth, we combined Sholl and branch order analysis to examine the changes in the branching pattern during development. One important measure for testing where new dendrites are added is the frequency distribution of branch order at different stages (Fig. 10A). During growth phase I (P4–P8), nodes are concentrated from branch order 1 to 40 (Fig. 10A), and the total number of branches increases within this range. In contrast, during growth phase II (P8–adult), a large proportion of nodes is added to the high branch order (40–80), whereas the number of nodes at the lower branch order (0–40) does not increase (in fact it appears to decrease). This finding indicates that, during growth phase II, most new branching occurs at the high branch order at the perimeter of the dendritic field.

To gather further support for this hypothesis, we analyzed the spatial distribution of nodes relative to the ADJ using the Sholl method (Fig. 10B) and determined how this distribution is changed during development (Sholl, 1953; see also Materials and Methods). From P1 to P4, the spatial distribution of the number of nodes changes very little, and most nodes are concentrated at a distance of 0 and 100 μm from the ADJ (not shown). From P5 to P8, the number of nodes is distributed evenly throughout the Sholl spheres between 20 to 180 μm, indicating the addition of new branches at multiple sites of the dendritic arborization. From stage P8 to adulthood, the most prominent increase of new nodes occurs at the perimeter of the dendritic field. For instance, about 400 new nodes are added in the Sholl distance range of 200–320 μm, indicating a period of mainly terminal branching (Fig. 10B). As shown in Figure 9, during growth, the mean dendritic length remains relatively constant. A stable MDL of all dendrites throughout pupal life could result either from a constant MDL throughout all branch orders and all stages or from an increase of MDL in low branch orders with a simultaneous increase of MDL in high branch orders, or vice versa. To distinguish between these possibilities, MDL was examined as a function of branch order in the major dendritic tree (Fig. 10C). During growth, the mean dendritic length remains relatively constant at increasing

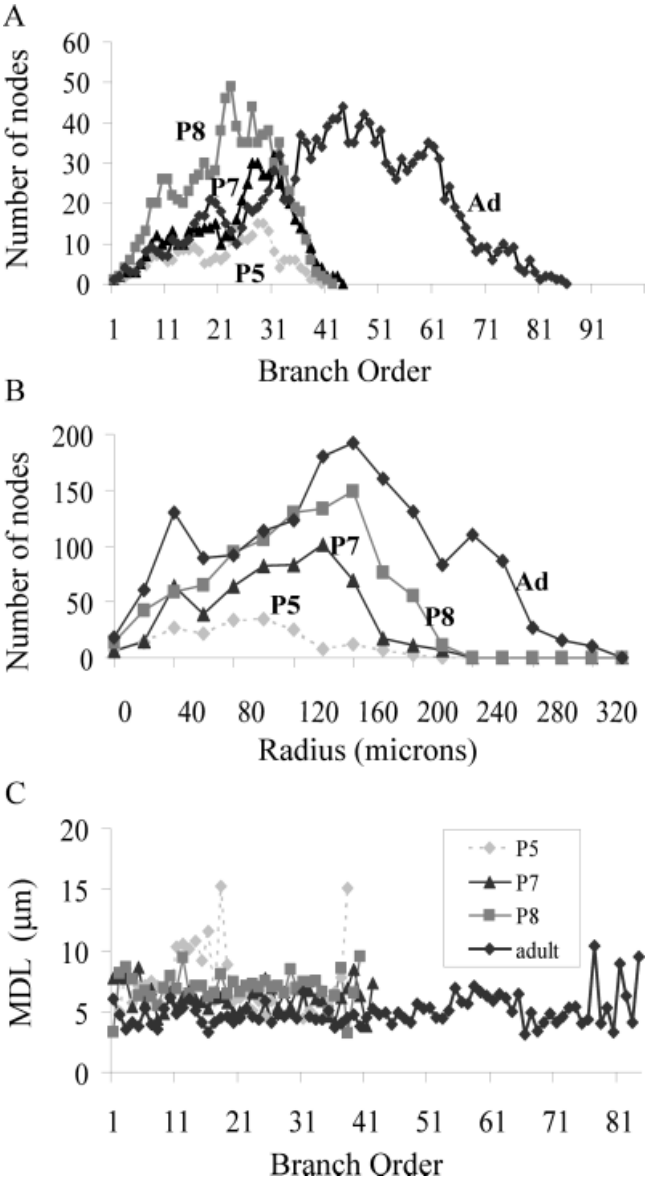

Fig. 10. Distribution of nodes using branch order analysis and Sholl analysis. **A:** Distribution of the nodes as a function of branch order during dendritic regrowth represented for four different developmental stages (P5, P7, P8, adult). Note the drastic increase in the number of high order branches between P8 and adult stages. **B:** The distribution of nodes along the dendritic field (Sholl analysis) is represented for the same four developmental stages (P5, P7, P8, adult) as in A. For that between the stages P8 and adult, numerous branches are added in the periphery of the dendritic tree, at a distance of 220–320 μm from the ADJ. **C:** Distribution of the mean dendritic segment length (MDL) as a function of branch order during dendritic regrowth shown for the same four developmental stages as in A and B (P5, P7, P8, adult).

branch orders throughout the tree for a given stage and changes little between stages. This further confirms that growth of the dendritic tree involves the addition of new dendritic segments (new nodes) without an elongation of the dendritic segments between nodes, regardless of the branch order.

DISCUSSION

Dendritic regression versus cell body growth

Late larval and early pupal life is characterized by drastic dendritic regression of MN5 with simultaneous growth of the cell body and the link segment. The eightfold decrease in dendritic surface area is due to a gradual loss of high order branches (orders 50–100) until the nodes are distributed in the branch orders 1–40 only. Although the mean length of all remaining branches is slightly decreased, retraction is mostly achieved by a reduction in the number of branches and not by shortening of the branches. The onset of dendritic regression and the parallel increase in the size of the cell body coincide in time with a brief increase in the systemic ecdysteroid titers, called the prepupal peak (Bollenbacher et al., 1981). For other *Manduca* motoneurons, it has been suggested that dendritic regression might be mediated by 20E (Weeks and Truman, 1985; Weeks, 1987; Weeks and Ernst-Utzschneider, 1989).

In *Drosophila* "broad-complex" mutants, in which the early ecdysone response genes are affected, cell body growth of motoneurons is decreased during early pupal stages (Consoulas, personal communication). Therefore, 20E is a likely signal for both dendritic regression and simultaneous cell body growth in MN5. This suggests that different cell compartments may respond differently to the same hormonal signal. A differential response to a single signal was also observed in oxytocin neurons of the supraoptic and the paraventricular nuclei (Stern and Armstrong, 1998) where lactation induces dendritic retraction with a simultaneous increase in the soma long axis and the soma surface area. A possible reason for an enlargement of the cell body during the retraction of dendrites is that the amount of dendritic membrane might be limited by intrinsic factors. In support of this hypothesis, in crickets, sensory deprivation induces dendritic growth of the medial dendrites and a concomitant decrease of the lateral dendrites of an auditory interneuron (Hoy et al. 1985). In the case of MN5, a possible mechanism for the expansion of the soma and the link segment might be membrane and cytoplasmatic incorporation from the regressing dendrites, but we have no experimental evidence for this hypothesis.

Ecdysteroid- induced formation of growth cones is a prerequisite for dendritic branching

The next 2–3 days (late P2 to early P4) of pupal development are characterized by the formation of dendritic growth cones. Neither the cell surface area, nor the number of branching points, nor the surface area of the cell body or the link segment is changed significantly during this time. This indicates that the formation of growth cones is a prerequisite for further dendritic growth and that growth of all central cell compartments is arrested during this phase. The formation of growth cones coincides with the rising phase of the second peak of systemic ecdysteroid titers (Bollenbacher et al., 1981). In vitro, 20E increases the complexity of growth cones (Matheson and Levine, 1999), suggesting that their formation in MN5 in vivo may be induced by the rising systemic ecdysteroid titers between the pupal stages P2 and P4.

Growth-cone formation is followed by a first phase of dendritic growth (stage P4–P8), during which the increase in surface area is associated with an increase in dendritic branching (number of nodes). In general, neuronal branching following growth-cone formation can occur in two different modes or a combination of both: growth-cone branching, which occurs either at the tips of the processes (splitting) or behind the growth cone (delayed branching; Acebes and Ferrus, 2000). In MN5 in vivo, the most rapid rate of increases in the number of dendritic branching points and surface area occurs during growth phase I, when growth cones are present at the tips of all dendrites. Although growth cones are rarely observed along the length of the dendritic branches, branch order analysis indicates the formation of new branches at lower branch orders from 1 to 20.

In addition, Sholl analysis indicates the presence of new nodes in the proximal portion of the dendritic tree at a distance range between 0 and 200 μm. This suggests that although splitting may prevail during growth phase I, some delayed branching occurs as well. As in several other in vitro systems (*Drosophila*: Kim and Wu, 1987; rat sympathetic and parasympathetic neurons: Bray, 1973; crayfish: Egid and Lnenicka, 1993), cultured *Manduca* motoneurons form new branches mostly at the growth-cone tip and 20E increases the number of branches added (Matheson and Levine, 1999). The rising ecdysteroid titer between the pupal stages P2 and P8 (Bollenbacher et al., 1981; Warren and Gilbert, 1986) may induce the rapid dendritic growth that is characteristic of growth phase I by enhancing growth-cone branching in a similar fashion as it does in vitro (Prugh et al, 1992; Matheson and Levine, 1999).

Putative signals for the growth of high order branches during late pupal life

In contrast to the rapid growth and branching characteristic for phase I, during phase II, the formation of new branches occurs in the absence of growth cones. Growth cones are present at the tips of the dendrites until pupal stage P6, and a few can occasionally be observed until pupal stage P8, but no growth cones are found at later stages. Therefore, the mode of dendritic field growth is qualitatively different during the second 50% of pupal development. In the absence of growth cones, neuronal branching can occur in two different modes or a combination of both: 1) formation of new branches at the terminals; or (2) interstitial or preterminal branching (Acebes and Ferrus, 2000). During growth phase II (P8–adult), a large proportion of nodes is added to high branch orders (40–80), whereas the number of nodes at lower branch orders (1–40) does not increase. (In fact it appears to decrease.) A decrease in the number of branches at lower branch orders (0–40) is incompatible with interstitial branching. Furthermore, the average segment length decreases little, and the distribution of the mean dendritic length (MDL) along the branch order stays constant as new branches are added. One should expect a major change in MDL if interstitial branching occurred. In addition, most new branches are added at the periphery of the dendritic field, as shown by the Sholl analysis. This indicates that terminal branching in high branch orders at the perimeter of the dendritic field occurs at a much higher rate than interstitial branching.

It appears plausible that, during the final structural refinement of MN5, the overall hormonal control might be replaced by more specific signals. High order branches at the perimeter of the dendritic field receive probably most of the synaptic input during the final integration of MN5 into the new flight motor circuits. Therefore, the contact with or the activity of presynaptic partners might induce the outgrowth of the high order branches. Deafferentation has been reported to cause reduction of specific portions of the dendritic tree of an identified motoneuron in *Manduca* (Kent and Levine, 1993) and prevents the formation of high order dendritic branches during dendritic maturation of cockroach cercal giant interneurons (Mizrahi and Libersat, in press).

In vertebrates' tectal neurons, branch addition and retraction govern the maturation of dendritic trees. There, a first phase of rapid growth and branching is followed by a second phase of slower growth (Cline, 2001), similar to our observations on MN5.During the second phase, branching occurs mostly at the tips of the terminal branches of the tree, and synaptic activity stabilizes dendritic structure (Cline, 2001). This further supports the hypothesis that, during growth phase II, the addition of high order branches to the perimeter of the dendritic field of MN5 might require synaptic activity. In MN5, the initial phase of strong dendritic growth is accompanied by a significant reduction in MDL. In contrast, in embryonic *Xenopus* retinal neurons, the percentage of short axonal branches decreases slightly, but the relative number of long branches increases significantly during the first 3 days of rapid new branch formation (Zou and Cline, 1996). This indicates that different types of neurons might follow different schemes in changing the average branch length during new branch formation.

Putative signals for the cessation of growth-cone branching

The cessation of both growth-cone branching and increases in cell body and link segment surface area might simply be due to the falling systemic ecdysteroid titers after pupal stage P8 (Bollenbacher et al., 1981). Alternatively, additional signals might be necessary for the collapse of growth cones and the cessation of soma growth. Interestingly, the switch between growth phases I and II coincides temporally with the occurrence of Ca^{2+} spikes in MN5, which are allowed by a delay of several days between the development of the adult Ca^{2+} currents and the subsequent increase in K^+ currents (Duch and Levine, 2000). These Ca^{2+} spikes occur spontaneously and can be evoked by sensory stimulation (Duch and Levine, 2000), suggesting that they occur during normal development. Furthermore, single calcium spikes lead to significant increases in the cytosolic calcium concentrations in the dendrites and the soma of MN5 (Duch and Levine, 2002). In culture systems, low levels of Ca^{2+} promote, but high levels of Ca^{2+} influx inhibit growth-cone extension and branching (Kater et al., 1988; Kater and Mills, 1991). During embryonic spinal cord development, Ca^{2+} elevations in the growth cones inhibit neuronal outgrowth, and large elevations in internal calcium occur at pausing sites (Gomez and Spitzer, 1999), causing an increase in the activity of calcineurin (Lautermilch and Spitzer, 2000).

In the developing *Xenopus* optic tectum, calcium/calmodulin-sensitive kinase II is required to limit neuronal growth (Zou and Cline, 1999). Thus, the Ca^{2+} spikes in

MN5 might function as stop signals for growth-cone branching by modulating Ca^{2+}-sensitive enzymes that affect the cytoskeleton. Blocking Ca^{2+} currents during normal development can test the possible role of Ca^{2+} entry in the cessation of growth-cone-mediated dendritic branching. Manipulating synaptic input to MN5 during normal development can test the possible role of synaptic interactions. Our morphometric database of MN5 will serve as a backbone to evaluate the effects of such manipulations to provide further insights into the control of dendritic development.

ACKNOWLEDGMENTS

We thank R.B. Levine and A. Mizrahi for editing and critical reading of the manuscript. The staining and imaging of neurons were performed in the laboratory of R.B. Levine at the University of Arizona, Tucson. The reconstructions and the morphometric analysis of neurons were performed in the laboratory of F. Libersat at Ben Gurion University, Beer Sheva. We thank Lior Rosenberg for help with the reconstructions of the neurons. F. Libersat was the recipient of grants 335/00-1 from the Israel Science Foundation and a grant from the Yael Foundation, R.B. Levine was the recipient of grant NS28495 from the NIH, and C. Duch was supported by fellowships from the Deutsche Forschungsgemeinschaft (DU 331/2-1 and DU331/2-2).

LITERATURE CITED

Acebes A, Ferrus A. 2000. Cellular and molecular features of axon collaterals and dendrites. Trends Neurosci 23:557–565.

Arnold AP, Gorski RA. 1984. Gonadal steroid induction of structural sex differences in the central nervous system. Annu Rev Neurosci 7:413–442.

Bell RA, Joachim FA. 1976. Techniques for rearing laboratory colonies of tobacco hornworms and pink ballworms. Ann Entomol Soc Am 69:365–373.

Bollenbacher WE, Smith SL, Goodman W, Gilbert LI. 1981. Ecdysteroid titer during the larval-pupal-adult development of the tobacco hornworm, *Manduca sexta*. Gen Comp Endocrinol 44:302–306.

Bray D. 1973. Branching patterns of individual sympathetic neurons in culture. J Cell Biol 56:702–712.

Bucher D, Scholz M, Stetter M, Obermayer K, Pflueger HJ. 2000. Correlation methods for three-dimensional reconstructions from confocal images: I. Tissue shrinkage and axial scaling. J Neurosci Methods 100:135–143.

Casadey GB, Camhi JM. 1976. Metamorphosis of flight motoneurons in the moth, *Manduca sexta*. J Comp Physiol [A] 112:143–158.

Catalano SM, Shatz CJ. 1998. Activity-dependent cortical target selection by thalamic axons. Science 281:559–562.

Cline HT. 2001. Dendritic arbor development and synaptogenesis. Curr Opin Neurobiol 11:118–26.

Consoulas C, Duch C, Bayline RJ, Levine RB. 2000. Behavioral transformations during metamorphosis: remodeling of neural and motor systems. Brain Res Bull 53:571–583.

DeVoogd T, Nottebohm F. 1981. Gonadal hormones induces dendritic growth in the adult avian brain. Science 214:202–204.

Duch C, Levine RB. 2000. Remodeling of membrane properties and dendritic architecture accompanies the postembryonic conversion of a slow into a fast motoneuron. J Neurosci 20:6950–6961.

Duch C, Levine RB. 2002. Changes in calcium signaling during postembryonic dendritic growth in *Manduca sexta*. J Neurophysiol 87:1415–1425.

Duch C, Bayline RJ, Levine RB. 2000. Postembryonic development of the dorsal longitudinal flight muscle and its innervation in *Manduca sexta*. J Comp Neurol 422:1–17.

Egid K, Lnenicka GA. 1993. Regeneration from crayfish phasic and tonic motor axons in vitro. J Neurobiol 24:1111–1120.

Fernandes JJ, Keshishian, H. 1998. Nerve-muscle interactions during flight muscle development in *Drosophila*. Development 125:1769–1779.

Gomez TM, Spitzer NC. 1999. In vivo regulation of axon extension and pathfinding by growth-cone calcium transients. Nature 397:350–355.

Gomez TM, Snow DM, Letourneau PC. 1995. Characterization of spontaneous calcium transients in nerve growth-cones and their effects on growth-cone migration. Neuron 14:1233–1246.

Gruenewald B, Levine RB. 1998. Ecdysteroid control of ionic current development in *Manduca* thoracic leg motoneurons. J Neurobiol 37:211–223.

Gu X, Spitzer NC. 1995. Distinct aspects of neuronal differentiation encoded by frequency of spontaneous calcium transients. Nature 375: 784–787.

Hoy RR, Nolen TG, Casaday GC. 1985. Dendritic sprouting and compensatory synaptogenesis in an identified interneuron follow auditory deprivation in a cricket. Proc Natl Acad Sci U S A 82:7772–7776.

Kammer AE, Rheuben MB. 1976. Adult motor patterns produced by the moth pupae during development. J Exp Biol 65:65–84.

Kater SB, Mattson MP, Cohan C, Connor J. 1988. Calcium regulation of neuronal growth. Trends Neurosci 11:315–321.

Kater SB, Mills LR. 1991. Regulation of growth cone behavior by calcium. J Neurosci 11:891–899.

Kent KS, Levine RB. 1993. Dendritic reorganization of an identified neuron during metamorphosis of the moth *Manduca sexta*: the influence of interactions with the periphery. J Neurobiol 24:1–22.

Kim YT, Wu CF. 1987. Reversible blockage of neurite development and growth cone formation in neuronal cultures of a temperature-sensitive mutant of *Drosophila*. J Neurosci 12:1382–1393.

Kurz EM, Sengelaub DR, Arnold AP. 1991. Androgens regulate the dendritic length of mammalian motoneurons in adulthood. Science 232: 395–398.

Lautermilch NJ, Spitzer NC. 2000. Regulation of calcineurin by growth cone calcium waves controls neurite extension. J Neurosci 20:315–325.

Levine RB, Weeks JC. 1996. Cell culture approaches to understand the action of steroid hormones on the insect nervous system. Dev Neurosci 18:73–86.

Mainen ZF, Sejnowski T. 1996. Influence of dendritic structure on firing pattern in model neocortical neurons. Nature 382:363–366

Matheson SF, Levine RB. 1999. Steroid hormone enhancement of neurite outgrowth in identified insect motoneurons involves specific effects on growth cone form and function. J Neurobiol 38:27–45.

Murphey DD, Segal M. 1996. Regulation of dendritic spine density in cultured rat hippocampal neurons by steroid hormones. J Neurosci 16:4059–4068.

Nijhout HF, Williams CM. 1974 Control of moulting and metamorphosis in the tobacco hornworm, *Manduca sexta* (L): growth of the last instar and the decision to pupate. J Exp Biol 61:481–491.

Penn AA, Shatz CJ. 1999. Brain waves and brain wiring: the role of endogenous and sensory-driven neural activity in development. Pediatr Res 4:447–458.

Prugh JK Della Croce, Levine RB. 1992. Effects of the steroid hormone, 20-hydroxyecdysone, on the growth of neurites by identified insect motoneurons *in vitro.* Dev Biol 154:331–347.

Reinecke JP, Bruckner JS, Grugel SR. 1980. Life cycle of laboratory reared tobacco hornworms, *Manduca sexta*, a study of development and behavior using time lapse cinematography. Biol Bull 158:129–140.

Riddiford LM. 1985. Hormone action at the cellular level. In: Kerkut GA, Gilbert LI, editors. Comprehensive insect physiology, biochemistry, and pharmacology, vol 8. New York: Pergamon. p 37–84.

Scott EK, Luo L. 2001. How do dendrites take their shape? Nat Neurosci 4:359–365.

Sholl DA. 1953. Dendritic organization in the neurons of the visual cortex and motor cortices of the cat. J Anat (Lond) 87:387–406.

Spitzer NC. 1991 A developmental handshake: neuronal control of ionic currents and their control of neuronal differentiation. J Neurobiol 22:659–673.

Spitzer NC, Gu X, Olsen E. 1994. Action potentials, calcium transients and the control of differentiation of excitable cells. Curr Opin Neurobiol 4:70–77.

Stern JE, Armstrong WE. 1998. Reorganization of the dendritic trees of oxytocin and vasopressin neurons of the rat supraoptic nucleus during lactation J Neurosci 183:841–853

Streichert LC, Pierce JT, Nelson JA, Weeks JC. 1997. Steroid hormones act

directly to trigger segment-specific programmed cell death of identified motoneurons in vitro. Dev Biol 183:95–107.

Tissot M, Stocker RF. 2000. Metamorphosis in *Drosophila* and other insects: the fate of neurons throughout the stages. Prog Neurobiol 62: 89–111.

Tolbert LP, Matsumotu SG, Hildebrand JG. 1983. Development of synapses in the antennal lobes of the moth, *Manduca sexta*, during metamorphosis. J Neurosci 3:1158–1175.

Uylings HBM, Ruiz-Marcos A, van Pelt J. 1986. The metric analysis of three-dimensional dendritic tree patterns: a methodological review. J Neurosci Methods 18:127–151.

Warren, JT, Gilbert LI. 1986. Ecdysone metabolism and distribution during the pupal-adult development of *Manduca sexta*. Insect Biochem 16:65–82.

Weeks JC. 1987. Time course of hormonal independence for developmental events in neurons and other cell types during insect metamorphosis. Dev Biol 124:163–176.

Weeks JC, Ernst-Utzschneider K. 1989. Respecification of larval proleg motoneurons during metamorphosis of the tobacco hornworm, *Manduca sexta*: segmental dependence and hormonal regulation. J Neurobiol 20:569–592.

Weeks JC, Levine RB. 1990. Postembryonic neuronal plasticity and its hormonal control during insect metamorphosis. Annu Rev Neurosci 13:183–194.

Weeks JC, Levine RB. 1995. Steroid hormone effects subserving behavior. Curr Opin Neurobiol 5:809–815.

Weeks JC, Truman JW. 1985. Independent steroid control of the fates of motoneurons and their muscles during insect metamorphosis. J Neurosci 5:2290–2300.

Zou DJ, Cline HT. 1996. Expression of constitutively active CaMKII in target tissue modifies presynaptic axon arbor growth. Neuron 16:529–539.

Zou DJ, Cline HT. 1999. Postembryonic calcium/calmodulin-dependent kinase II is required to limit elaboration of presynaptic and postsynaptic neuronal arbors. J Neurosci 19:8909–8918.